HHS Public Access

Author manuscript

Med Phys. Author manuscript; available in PMC 2023 March 01.

Published in final edited form as:

Med Phys. 2022 March ; 49(3): 2068–2081. doi:10.1002/mp.15129.

Model studies of the role of oxygen in the FLASH effect

Vincent Favaudon[1,*], **Rudi Labarbe**[2], **Charles L. Limoli**[3]

[1]Institut Curie, Inserm U 1021- CNRS UMR 3347, University Paris-Saclay, PSL Research University, Centre Universitaire, 91405 Orsay Cedex, France.

[2]Ion Beam Applications S.A. (IBA), Louvain-la-Neuve, Belgium.

[3]Dept. of Radiation Oncology, Medical Sciences I, B146B, Irvine, California 92697-2695, USA.

Abstract

Current radiotherapy facilities are standardized to deliver dose rates around 0.1-0.4 Gy/s in 2 Gy daily fractions, designed to deliver total accumulated doses to reach the tolerance limit of normal tissues undergoing irradiation. FLASH radiotherapy (FLASH-RT) on the other hand, relies on facilities capable of delivering ultrahigh dose rates in large doses in a single microsecond pulse, or in a few pulses given over a very short time sequence. For example, most studies to date have implemented 4-6 MeV electrons with intra-pulse dose rates in the range 10^6-10^7 Gy/s. The proposed dependence of the FLASH effect on oxygen tension has stimulated several theoretical models based on three different hypotheses: (i) Radiation-induced transient oxygen depletion; (ii) Cell-specific differences in the ability to detoxify and/or recover from injury caused by reactive oxygen species; (iii) Self-annihilation of radicals by bimolecular recombination. This article focuses on the observations supporting or refuting these models in the frame of the chemical-biological bases of the impact of oxygen on the radiation response of cell free, *in vitro* and *in vivo* model systems.

Keywords

FLASH radiotherapy; Oxygen; Peroxyl radicals; Radical recombination

1 INTRODUCTION

A novel delivery modality named “FLASH” radiotherapy (FLASH-RT) has emerged recently[1]. Whilst radiotherapy facilities are currently set to deliver dose rates around 0.05-0.40 Gy/s (CONV) in 2 Gy daily fractions accumulated to reach the tolerance limit of normal tissues undergoing irradiation, FLASH-RT relies on ultrahigh dose rate facilities and consists of delivering a large dose in a single microsecond pulse, or in a few pulses given over a very short time. FLASH-RT was established using 4-6 MeV electrons with intra-pulse dose rates in the range 10^6-10^7 Gy/s[1] and was found to spare the lung of C57BL/6J mice exposed to 15 Gy by bilateral thorax irradiation from radiation-induced

*Corresponding author: vincent.favaudon@curie.fr.

Competing interests: The authors have no conflicts to disclose.

fibrosis whilst preserving the antitumor efficacy in xenografted as well orthotopic, syngeneic models[1]. These features have been confirmed by other teams in adult and juvenile mouse brain, mouse tail, mouse and pig skin, cat muzzle, zebrafish and mouse intestine (for a review see the article “Radiobiology of the FLASH effect” in the same issue of the journal). Research groups investigating the feasibility of FLASH-RT with proton beams[2] have found promising results, with gut sparing from necrosis after 18 Gy 230 MeV protons FLASH-RT delivered at 78 Gy/s[3] and reduced lung fibrosis and skin dermatitis after proton FLASH exposures at 40 Gy/s[4].

Corroborating observations made 39 years ago with mouse tail necrosis as an endpoint[5], Montay-Gruel *et al.* recently demonstrated that sparing the adult and juvenile mouse brain from radiation-induced gliosis, loss of neural stem cells and impaired memory by ultrahigh dose rate irradiation is, at least in part, an oxygen-dependent process[6,7]. In support of this idea, carbogen breathing was found to reverse the neuroprotective effect of FLASH-RT[6]. In addition, brain studies allowed to establish the minimal dose/dose rate requirements for the FLASH effect to persist in this organ; here data pointed the dissolution of the FLASH effect in brain as the intra-pulse dose rate was < 30 Gy/s and the total treatment time > 300 ms[8]. Furthermore, available experimental data show that the FLASH effect depends on the intra-pulse dose rate and, when multiple pulses are used, on the time interval between pulses and the overall duration of FLASH radiation exposure[9-12].

These dose-rate characteristics and the discovery of the oxygen dependence of the FLASH effect, have stimulated several theoretical models based on three different hypotheses, namely:

(i) Radiation-induced transient oxygen depletion (TOD).

(ii) Cell-specific differences in the ability to detoxify and/or recover from injury caused by reactive oxygen species.

(iii) Self-annihilation of radicals by bimolecular recombination.

This article will focus on the different observations (summarized in Table 1) that underpin these models in the frame of the chemical-biological bases of the impact of oxygen on radiation response, and in light of novel findings regarding DNA damage and survival under FLASH-RT conditions.

2 CHEMISTRY OF PEROXYL RADICALS AND THEIR IMPACT ON RADIATION RESPONSE

This section reviews the involvement of oxygen in radiochemistry in cells and tissues at conventional dose rate.

2.1 Discovery of the oxygen effect

Schwarz[13] was the first to establish that cells irradiated in anoxia are less sensitive to ionizing radiation than if irradiated in the presence of O_2. Using vegetable seeds, Petry[14]

established a correlation between radiosensitivity and the presence of O_2. Ten years later Crabtree and Cramer[15] reached similar conclusions using tumor slices. Years later Read[16] and Gray *et al.*[17] provided the first quantitative determination of the *Oxygen Enhancement Ratio* (OER) on radiation survival.

Oxygen increases the radiation susceptibility of cells with a maximum OER between 2.5 and 3.5[18]. It is thus conceivable that a low concentration of oxygen, such as found in hypoxic domains located far from the wall of arterioles[19], protects tissues from radio-induced damage. On the other hand, it has long been reported[20,21] that the OER for cell killing presents a discontinuity between 1 and 10 μM oxygen. This finding has rarely been taken into consideration and it is usually assumed that the dependence of cell killing on the partial pressure of O_2, is continuous. Consistent with Tallentire *et al.*[20] and Millar *et al.*[21], however, Ewing and Powers[22] and Kiefer *et al.*[23] proposed a three-way mechanism to explain the effect of oxygen on bacterial spores and concluded that one into three of these mechanisms only depends on the $^{\bullet}OH$ radical. Other authors also suggested that the oxygen effect is subdivided into two or more processes[21,24].

2.2 Mechanism of the oxygen effect - The peroxyl radicals ROO$^{\bullet}$

The radiosensitizing effect of oxygen[18,25] has long been known to stem from peroxyl radicals ROO$^{\bullet}$ [26]. Peroxyl radicals are formed by addition of O_2 to short-lived, “primary” carbon-centered radicals (R$^{\bullet}$) generated upon H$^{\bullet}$ atom abstraction from aliphatic or unsaturated substrates RH (Figure 1). This idea was critically tested by the fast mixing techniques developed by Howard-Flanders and Moore[27] and later by Michael *et al.*[28]. Their work showed that R$^{\bullet}$ fades away in complete absence of O_2 with a half-reaction time of 500 μs in bacteria[27,28] and less than 5 ms in mammalian cells[29,30]. Consistently, past 10 ms following irradiation the susceptibility of cells to radiation is independent of the presence of oxygen[31].

Carbon-centered radicals R$^{\bullet}$ may evolve through four paths, namely (Figure 2):

- **i.** Restitution of RH by electron transfer from reduced glutathione or other hydrogen donors.
- **ii.** Self-decomposition, eventually with C-C bond breakage.
- **iii.** Self-inactivation by radical-radical recombination.
- **iv.** Oxygen capture yielding peroxyl radicals ROO$^{\bullet}$.

With the exception of certain purine-derived radicals[32,33], carbon-centered radicals R$^{\bullet}$ are prone to readily combine with O_2 to form peroxyl radicals ROO$^{\bullet}$. The *rate constant* (k) for addition of oxygen entails virtually no activation barrier and in solution may be as high as $2\ 10^9\ M^{-1}.s^{-1}$. k is likely to be several orders of magnitude lower in cells or tissues, because of steric hindrance, or restricted diffusion in relation to viscosity. The *velocity* of the reaction, i.e., the product of k by the concentrations, $V = k.[R^{\bullet}].[O_2]$, may also be limited by a low availability of O_2. In bacterial and mammalian cells we would approximate k to $\leq 5 \times 10^7 M^{-1}.s^{-1}$ [29,34,35].

2.3 Fate and reactivity of ROO• radicals

ROO• radicals are generally thought to represent a non-restorable form of the target molecule. However, ROO• is not the end-product of the reaction of R• with O_2. Although the C-O-O bond is stable at room temperature[36,37], ROO• radicals are highly reactive and prone to undergo unimolecular or bimolecular decay including initiation of peroxidative chain reactions[38]. Oxygen isotopic labeling has shown that the decay of organic ROO• radicals in solution involves a short-lived tetroxide intermediate evolving through several pathways with the elimination of $^1O_2$, H_2O_2 or HO_2•.

2.3.1 Nucleobases and DNA.—In pyrimidines or 2'-deoxyribose, ROO• radicals end in peroxides, glycols, ketones or bond breakage (for a review see[39]). The relative probability of unimolecular *vs.* bimolecular processes depends on the probability of encounter, hence on the mobility of the molecules of interest. In solution the probability of intramolecular rearrangements is low compared to the tetroxide pathway. Rearrangements through this pathway frequently involve release of superoxide, H_2O_2 or O_2. Conversely, uptake of a second molecule of O_2 may occur. The deoxyribose moiety is also prone to radiation-induced cleavage, frequently involving release or uptake of a second molecule of O_2, or release of superoxide that disproportionates into O_2 and H_2O_2 [39].

The fate of the ROO• radical within the DNA double helix is dependent on the neighbouring environment. An example is provided by the abstraction of a hydrogen atom from a deoxyribose residue by a vicinal dihydropyrimidine peroxyl radical[40]. This reaction produces two contiguously damaged nucleotides which may also lead to a strand break[41]. Specifically, the 5,6-dihydropyrimidine peroxyl radical may covalently add to 5'-adjacent nucleobases, with a preference for the C8 of deoxyguanosine leaving 8-hydroxy-2′-deoxyguanosine (8-OHdG)[42-44] (Figure 2). Such “tandem” damage has attracted considerable interest because of its capacity to inhibit DNA repair due to inefficient removal by glycosylases, leading to local accumulation of DNA double-strand breaks. Whether FLASH-RT reduces this type of DNA damage has not yet been demonstrated, but represents an attractive hypothesis that warrants further investigation.

2.3.2 Lipids.—Peroxyl radicals are powerful oxidants able to catalyze chain reactions. The best example comes from peroxidation of unsaturated phospholipids in membranes. The radiolytic yield of peroxyl radicals in these lipid-based pathways may be high, and is in proportion to the length of the chain. The chain length is maximal at low dose rate and decreases in inverse proportion to the square root of the dose rate (see section 3.3). Chain propagation may be minimal at large doses given at ultrahigh dose rate, due to self-recombination of the primary (R•) or secondary radicals (ROO•). Note again that these mechanisms rely on the probability of collision between free radicals, and hence on their relative mobilities.

The most common byproducts of lipid peroxidation involve thiobarbituric acid reactive substances, alkenals and isoprostanes (Figure 2). As alluded to above, ROO• radicals are prone to decay through tetroxide intermediates involving release of superoxide and oxygen[39,45]. This process limits transient oxygen depletion (TOD) occurring early after

FLASH-RT *via* the reduction of O_2 into superoxide by e_{aq} and $H^{\bullet}$, as well as the activation of redox-sensitive proteins or Fenton-like reactions (for a review see[46]).

Increased permeability to Na^+ or K^+, alteration of active transport, loss of sulfhydryl function, altered lipid metabolism and decoupling of the electron transport chain in mitochondria, have long been considered as major outcomes of membrane damage after ionizing radiation. Other data suggesting that oxidative deterioration of phospholipids is involved in aging, degenerative diseases and even cell lethality[47] further support the importance of membrane targets. Nonetheless, the role of lipid peroxidation has been questioned[48], as modification of the polyunsaturated lipid content in the plasma membrane was not found to alter radiation susceptibility[49]. However, radiation-induced activation of sphingomyelinases initiating the release of ceramides in response to peroxidation of unsaturated phospholipids, has emerged as an important pro-apoptotic and pro-inflammatory pathway[50-53]. Moreover, among the many products derived from the peroxidation of unsaturated lipids, certain species such as alkenals, are highly reactive and able to form mutagenic or lethal covalent adducts with DNA or chromatin[47,54,55].

2.4 Biological consequences of lipid peroxidation with regard to DNA damage

Interestingly, by virtue of their long half-lives (≥ 10 s according to Pryor *et al.*[56] and Phaniendra *et al.*[57]), lipid-derived peroxyl radicals generated at phospholipid membranes are able to attack DNA far from their site of formation. 8-OHdG, one of the major mutagenic products of oxidative DNA damage, was identified by Hruszkewycz *et al.*[58] in the DNA of isolated mitochondria after treatments to induce peroxidation of phospholipid membranes. 8-OHdG was also identified as a byproduct in calf thymus DNA exposed to liposomes under peroxidative conditions[59]. Interestingly, Goto *et al.*[60] demonstrated that the formation of 8-OHdG by lipid peroxyl radicals requires the presence of deoxythymidine and is mediated by 5-(hydroperoxymethyl)-2-deoxyuridine, the main peroxidized product of 2'-deoxythymidine. This study sheds light onto the mechanisms involved in lipid peroxyl radical-induced oxidative damage to nucleobases. Data suggests a two step reaction, namely, peroxidation of deoxythymidine into 5-(hydroperoxymethyl)-2′-deoxyuridine by a lipid peroxyl radical, followed by internal transfer between adjacent deoxyguanosine within the DNA double helix.

In conclusion, a wealth of studies to date demonstrate the capability of ionizing radiation exposure to elicit a wide-range of phopholipid damage able to initiate chain propagating reactions through peroxyl radical intermediates that may eventually lead to oxidative damage to DNA. Whether such reactions are stabilized, inhibited or promoted upon FLASH-RT conditions remains to be seen, but further studies evaluating the nuances of lipid peroxidation chain reactions may provide considerable insight into the mechanisms underlying the FLASH effect.

3 COMPUTATIONAL MODELS OF THE FLASH EFFECT IN RELATION TO OXYGEN

In this section, several models attempting to explain the effect of dose rate on oxygen chemistry in cells are presented. As mentioned by Wardman[61], based on the knowledge acquired during 60 years of pulse radiolysis in solution, two hypotheses (among others) can be proposed to explain the differences observed at CONV *vs.* FLASH-RT dose rate: *(i)* depletion of O_2 critical to the biological response to radiation due to a competition between the depletion rate and the rediffusion rate of the species from the capillaries, or *(ii)* increased probability of radical-radical recombination under FLASH-RT conditions due to transient accumulation of a large concentration of radical species during a short time window.

These two hypotheses can be framed in a consistent mathematical model linking radiochemical and biochemical reaction networks represented in Figure 2. In one instance, the TOD hypothesis assumes that at ultrahigh dose rate the oxygen concentration is sufficiently decreased to change the dynamics of the network. In contrast, the self-annihilation of radicals hypothesis (labelled *(ii)* in Section 1 and in Figure 2 and described in section 3.2) suggests that, at ultrahigh dose rates, the competition between the second order recombination of carbon-centered ($R^{\bullet}$) and the reaction of $R^{\bullet}$ with oxygen is the mechanism predominating under these conditions.

Whatever hypotheses, when 10 Gy are delivered at a time-averaged dose rate > 40 Gy/s (FLASH-RT), the total radiation time is < 0.25 s. Furthermore, the FLASH effect has been observed with pulsed electron beams and with a virtually continuous proton beam[3]. The main difference between CONV and FLASH-RT dose rates is likely to involve processes taking place on a time scale on the order of milliseconds to seconds. This is consistent with the approach of Spitz *et al.*[62] who focused on chemical and biochemical reactions occurring over these rapid time scales. The processes taking place during the physical and physico-chemical steps of radiochemistry, *i.e.,* within 1 μs after the initial physical event, can probably be ignored as already suggested by Vozenin *et al.*[63] (see Fig. 2 in that article). Electron track ends produce spurs and blobs of ionizations that can lead to high local concentration of radicals, yet the radiation doses used in FLASH-RT studies reported so far are not high enough for track overlap to be significant[61,64] and the initial radiation chemistry is similar in CONV and FLASH-RT modalities, with equivalent yields of radicals (G-values) escaping track recombination events in the first 10^{-7} s after ionization. To the extend that this is accurate, then detailed processes occurring on time scale shorter than 1 μs can be dismissed in favor of models using known G-values (at 1 μs) per radical species for CONV and FLASH-RT and detailing the homogeneous radiochemical reactions using standard chemical kinetic equations. However, data from Acharya *et al.*[9] at dose rates as high as $3x10^8$ Gy/s are consistent with additional radical-radical recombination events at the submicrosecond time scale. Resolution of these ideas must await further experimentation.

3.1 Transient Oxygen Depletion (TOD) model

The TOD model is based on a detailed analysis of the reaction rate of oxygen and of its rediffusion rate from capillaries. These 2 parameters will be reviewed in turn in this section.

In pure water in equilibrium with air, the concentration of dissolved O_2 is close to 200 μM. The reduction of O_2 into the superoxide anion $^{\bullet}O_2^-$ by electron transfer from e_{aq} and $H^{\bullet}$ occurs at the microsecond time scale with a radiolytic yield G = [G(e_{aq}) + G($H^{\bullet}$)] = 0.342 μM/Gy.

Partial consumption of O_2 thus occurs instantly in proportion to the dose of radiation. Regeneration of O_2 by dismutation of $^{\bullet}O_2^-$ is slow at neutral pH ($2k \leq 0.35\ M^{-1}.s^{-1}$). H_2O_2 thus generated adds to the amount (G = 0.073 μM/J) formed by recombination of $^{\bullet}OH$ radicals during the elementary processes of water radiolysis. In cells regeneration of O_2 from $^{\bullet}O_2^-$ and H_2O_2 is accelerated by superoxide dismutases and catalases, respectively.

Pioneering works showed that when bacteria (reviewed in Epp *et al.*[34]) or mammalian cells[65] were exposed to submicrosecond, single pulses of relativistic electrons, clonogenic survival curves at high doses turned out to be parallel to those for cells maintained under anoxia. Based on studies with radioresistant bacteria this feature was initially attributed to radiation-induced depletion of free O_2 in the cytoplasm within a time shorter than oxygen replenishment occurring by diffusion from the medium to cells[66]. With mammalian cells, however, this effect was observed at very low pO_2 only, typically < 0.5%[65,67]. Under these conditions the percentage of oxygen depletion in the culture medium may be significant, in proportion to the doses applied. However, it is difficult to make a decision on the contribution of intracellular O_2 depletion *vs.* reduced availability of oxygen in the environment of cells, all the more so intracellular trapping of O_2 by long-lived, non-lethal free radical species may render oxygen molecules unavailable for addition to critical sites in target cells[68].

To estimate the amount of oxygen depletion in mammalian cells, Spitz *et al.*[62] used the radiolytic yields of e^-_{aq} and $H^{\bullet}$ known from pulse radiolysis studies in pure water to calculate the amount of superoxide anion produced in a pulse, then took into consideration the action of superoxide dismutase, the decomposition of superoxide *via* Fenton reaction, and the reaction of $^{\bullet}OH$ with organic molecules to form carbon centered radicals that subsequently react with oxygen to form $ROO^{\bullet}$ radicals. The authors considered the chain propagation reaction $ROO^{\bullet}$ + RH and the chain termination, such as the reaction of $ROO^{\bullet}$ with vitamin E and estimated that the total oxygen concentration consumed by all those reactions would be around 25 μM for a dose of 10 Gy. They also expected that reactions of superoxide with Fe-containing proteins release labile iron (Fe^{2+}) and could double or even triple the size of the intracellular redox active labile iron pools at the time of the FLASH-RT run. This labile Fe^{2+} would be available to participate in damaging Fenton-type reactions. As tumor cells, relative to normal cells, have 2- to 4-fold higher levels of labile iron, the process could greatly magnify free radical chain reactions in tumor tissues exposed to FLASH-RT (relative to normal tissues), leading to significantly higher levels of organic hydroperoxide and oxidative damage in cancer cells.

Pratx and Kapp[69] used an oxygen depletion rate of 0.42 mm Hg/Gy (= 0.75 μM/Gy) as reported in the literature. Based on the oxygen enhancement ratio, they showed that for a 10 Gy dose, one expects a 30% decrease in radiosensitivity, due to oxygen depletion if the initial oxygen concentration was 5 mm Hg (8.9 μM); no decrease in radiosensitivity was

expected if the initial oxygen concentration was above 20 mm Hg (36 μM). These results are comparable to those of Petersson et al.[67,70] . Given that the oxygen tension in normal tissues is between 150 μM in arterial and 40 μM in venous blood, the models of Pratx and Petersson would suggest that oxygen depletion alone is not sufficient to explain why normal tissues are spared from radio-induced complications under FLASH-RT conditions.

Some TOD models[62,67,69-72] use a “static” approach that considers the amount of oxygen consumed after delivering 10 Gy in competition with replenishment from oxygen diffusion out of blood vessels, but without explicitly taking into account the kinetics of the radical reactions nor the time structure of the FLASH-RT beams. The dynamic nature of the "oxygen effect" in the micro-millisecond time range is ignored, which could be a strong limitation as noted by Wardman[61]. In support of the TOD model, in bacteria and eukaryotic cells grown under low pO_2, it was earlier reported by Dewey and Boag[66] that reduction of oxygen by e_{aq} and $H^{\bullet}$ may lead to complete consumption of free O_2 in the cytoplasm giving rise to broken survival curves when large doses of radiation were given within a time shorter than oxygen replenishment by diffusion from the medium to cells (reviewed in Epp *et al.*[34]), consistent with the lifetime of carbon-centered radicals formed from the radiolysis setup (see section 2.2). These observations are at the root of the Transient Oxygen Depletion (TOD) model, but clearly measured under conditions distinctly different than the *in vivo* environment that defines the FLASH effect, a point worth re-emphasizing.

Moreover, a debate is ongoing as to whether extensive, radiation-induced oxygen depletion actually occurs in tissues *in vivo*. Firstly, in disagreement with the TOD model, available data[19,73-75] suggest that the oxygen tension in normal lung is too high to support significant depletion of O_2 at the doses used to initiate fibrosis[1]. The effects observed in human lung fibroblasts and stem cells cultivated *in vitro* in equilibrium with 200 μM O_2 and exposed to 2-5 Gy[76] as well as earlier cytogenetic studies[9,77,78] are also inconsistent with the TOD model. Secondly, the models may overestimate the radiolytic yield of $^{\bullet}O_2^-$ when it considers the tissue response to FLASH-RT. Actually, the scavenging activity of the cytosol towards all radicals is high, and the amount of $H^{\bullet}$ and e_{aq} acceptors is elevated such that the radiolytic yield of $^{\bullet}O_2^-$ inside a cell is likely smaller than in pure water by an order of magnitude. Furthermore, in an aqueous cell suspension the radicals formed in the bulk medium (exogenous) have little biological impact compared to radicals formed within the cell (endogenous)[79]. On the other hand, the basal cytosolic steady-state amount of H_2O_2 can rise transiently to 0.5-0.7 μM during oxidative signaling events. Thus, in comparison to metabolic H_2O_2 production, the radiolytic yield of H_2O_2 is low and unlikely to challenge cellular defenses. Based on the foregoing, low yields of radiolytic H_2O_2 appear insufficient to account for the isoefficiency of tumor cell kill between CONV and FLASH-RT conditions. Last but not least, Cao *et al.*[80] performed direct measurements of oxygen consumption in irradiated samples *in vitro* and *in vivo* exposed to 10 MeV electrons at 0.1 (CONV) *vs.* 300 Gy/s (FLASH) using phosphorescence quenching by oxygen of the water-soluble probe Oxyphor 2P. The results showed that oxygen depletion down to hypoxic levels is unlikely to occur. These results have been confirmed under similar dose rate conditions by Jansen *et al.*[81] in sealed water phantoms using a fiber-optic FireStingO2 oxygen microsensor. Moreover, less oxygen depletion per dose was observed under FLASH-RT compared to CONV conditions by both authors. Therefore, the total amount of oxygen

depleted upon irradiation at the maximum doses used in FLASH-RT studies, is definitely too low to account for the FLASH effect in normoxic tissue.

Let's now consider the rate of oxygen rediffusion. Petersson *et al.*[70] developed an analytical model of the reaction rate of O_2 consisting in two competing terms: *(i)* the $[O_2]$ depletion rate which is proportional to the dose rate and the instantaneous $[O_2](t)$ and *(ii)* the re-oxygenation rate which is proportional to the difference between the instantaneous $[O_2](t)$ and the oxygen concentration in the environment. By integrating the rate equation, one obtains $[O_2](t)$ as a function of time during irradiation at constant dose rate. If "oxygen depletion" means that the molecular oxygen is radio-converted into species that are harmless to the cells, one can then predict the oxygen enhancement ratio (OER) from the residual molecular oxygen concentration ($[O_2](t)$). The model parameters were obtained by a fit to the experimentally measured survival fraction of prostate cancer cells grown in monolayer culture and irradiated under different oxygen concentrations with different doses and dose rates[67]: under normoxic conditions, there were no differences between FLASH-RT and CONV irradiation whilst, for moderately hypoxic cells (initial $[O_2] = 21.6\mu M$), the radiation response was similar up to a dose of about 5–10 Gy, above which increased survival was observed for FLASH-RT dose rates.

Several groups have also explicitly taken into account the oxygen rediffusion from the capillary by solving Fick's diffusion equation numerically in a finite element model[82] or analytically[69]. In those models, the reactions of oxygen consumption are not as detailed as in Spitz *et al.*[62]. Rothwell *et al.*[82] introduced the effective diffusivity (D_{eff}) of oxygen to account for the porous nature of space between cells filled with an extracellular matrix and non-linearity of the path traversed by diffusing molecules relative to an obstacle-free medium. D_{eff} can be one order of magnitude smaller than the molecular diffusivity of oxygen, therefore slowing down the oxygen diffusion. Rothwell *et al.*[82] also included a metabolic reaction rate (Michaelis-Menten type) and a radiolytic reaction (first order in oxygen concentration) and did a sensitivity study of the model predictions with the rate constants value to show that a FLASH-RT behavior can be reproduced by the model. However, one may wonder whether the value of rate constant giving the behavior in question are biologically sensible.

3.2 Model based on the ability to detoxify from reactive oxygen species

In contrast to normal cells, cell survival and DNA damage recognition and repair[76] of tumor cells appear to be similar under CONV and FLASH conditions, with one exception reported to date[83]. While normal tissue sparing and isoefficient tumor kill define the FLASH effect, the differential response of normal tissue and tumors to FLASH irradiation may involve inherent differences in the ability to detoxify reactive oxygen species and resultant byproducts. To account for this, Spitz et al.[62] suggested that, relative to tumor cells, normal cells have lower pro-oxidant burdens during normal steady-state metabolism but a greater reserve capacity for the enzymatically mediated elimination of peroxidized compounds. More efficient elimination of organic hydroperoxides and reduced levels of labile iron that promote damaging Fenton-chemistry may foster detoxification of reactive oxygen species and reduce oxidative injury in normal tissue compared to tumors, that in

part, provide one plausible explanation for the normal tissue sparing afforded by FLASH-RT. Cell lines constructed to over-express and eliminate key antioxidant enzymes (GPX1, GPX4, Catalase, etc.) provides a means for critically testing these hypotheses *in vitro*, while analogous strategies using transplanted tumors and transgenic mouse models provide tractable approaches *in vivo*.

3.3 Self-annihilation of radicals by bimolecular recombination

To construct a numerical model of the reaction network kinetics Labarbe *et al.*[84] considered the mechanisms suggested by Spitz *et al.*[62], namely, superoxide formation and dismutation, oxygen consumption along chain reactions initiated by formation of peroxyl radicals, Fenton reactions and restoration of oxygen from tetroxide intermediates in chain termination and from H_2O_2 by catalase. The fate of lipid and DNA peroxyl radicals, as detailed in Section 2, can be represented by simple kinetic equations.

The model relies on the numerical resolution of a system of ordinary differential equations (ODE) describing the dynamic nature of the reactions of 9 chemical species (e^-_{aq}, O_2, H_2O_2, $^{\bullet}OH$, $H^{\bullet}$, H_2, $O_2^{\bullet-}$, $R^{\bullet}$ and $ROO^{\bullet}$) to predict the time-dependent evolution of their concentrations. The temporal structure of the irradiating pulses ($\frac{dD(t)}{dt}$) was included in the ODE. The G-values at 1 μs post-irradiation were used to convert the dose rate into the production rates of chemical species. The rate-constants values representative of cellular environments were found in the literature. The definition of the boundary conditions for the integration of the ODE allowed one to define the initial O_2 concentration.

A competition occurs between self-recombination ($R^{\bullet} + R^{\bullet} \rightarrow$ Non-Radical Products) of the "primary" carbon centered radical $R^{\bullet}$ and oxygen addition ($R^{\bullet} + O_2 \rightarrow ROO^{\bullet}$) (Figure 2). As noted by Wardman[61], short pulses of radiation at ultrahigh dose rate will generate a higher transient concentration of free radicals within a shorter time interval than for the CONV dose rate. The rates of the reaction of $R^{\bullet}$ with oxygen are proportional to the radical concentration (first order), but the rate of radical–radical recombination is proportional to the square of the radical concentration (second order). As the dose rate increases and the transient $[R^{\bullet}]$ increases, the rate of radical recombination increases proportionally more than the rate of reaction with oxygen. Actually, by solving the ODE for different irradiation conditions, the model predicts that under FLASH-RT conditions there is more $R^{\cdot}$ recombination and less production of tissue-damaging $ROO^{\cdot}$. Finally, in cells a substantial part of O_2 is likely to be consumed *via* the formation of transient peroxyl radicals ($ROO^{\cdot}$) formed at different time points. A portion of peroxyl radicals can dissociate into $^1O_2$, $^3O_2$ or $^{\bullet}O_2^-$ and thus partially resupply O_2 as discussed in Section 2. All these reactions are included in the model.

Peroxyl radicals $ROO^{\cdot}$ are known to be a major cause of detrimental effects throughout all cellular compartments, both as damaged species and damaging intermediates (see Section 2 above). Labarbe *et al.*[84] have speculated that exposure of cells to $ROO^{\cdot}$ is correlated to the level of bulk cellular damage represented by the "area-under-the-curve" (AUC) of the $[ROO^{\cdot}]$ over time. The model makes some quantitative predictions that can be compared to experimental results. Firstly, for a 10 Gy dose, $[O_2]$ decreases by < 3 μM, in good agreement

with Weiss *et al.*[85] and Koch[64] who reported a radiation-induced oxygen consumption of 0.45 μM/Gy. This suggests that oxygen consumption is not the key factor in explaining the FLASH effect. This conclusion is in line with Berry[86] and further with Koch's observation[64] that oxygen consumption by 10 Gy over a time frame of 250 ms is less than normal-tissue oxygen consumption by biological processes. Secondly, the model predicts a correlation between the cells' exposure (AUC) to peroxyl radicals $ROO^{\cdot}$ and the dose rate, dose and initial $[O_2]$ altogether, that could qualitatively explain the experimentally observed FLASH effect. Reassuringly, the model predicts that AUC depends on $^{1}/\sqrt{^{dD}/_{dt}}$, like the radiolytic yield dependence observed in unsaturated phospholipids auto-oxidation[26,38,87]. Thirdly, the model predicts a dose modifying factor around 1.4 (ratio of the dose at FLASH-RT dose rate to the dose at CONV dose rate leading to the same NTCP), consistent with published observations[1,8,76].

The kinetic model of radical recombination presents certain limitations. Firstly, whilst the reaction rate constants published in the literature were measured in homogeneous solution, their values in the cytosol and interstitial tissues are subject to large uncertainties. For example, scavenging of e^{-}_{aq} and $H^{\cdot}$ by the wealth of acceptors present in the cell could be much higher than the value used in the model, leading to a negligible net amount of e^{-}_{aq} and $H^{\cdot}$ available for reactions with O_2. The sensitivity of model predictions to uncertainty in rate constant values and free radical concentrations is a topic under investigation.

Secondly, only the kinetics of a limited number of biochemical reactions could be modelled, for lack of available data relating to spatial distribution, steric hindrance, viscosity, enzyme concentration, pH, and ionic strength. Further, the model does not discriminate between proteins, DNA, RNA, lipids, as all intracellular moieties are modelled by a single RH species. The model therefore misses the fact that some radicals could show a higher affinity for specific substrates, e.g., nucleobases or highly-reactive amino acid residues such as disulfide bonds, effects that could vary greatly between different biological compartments, especially those rich in unsaturated, aromatic and otherwise reactive macromolecular constituents.

Thirdly, the model does not account for spatial concentration gradients within defined cellular compartments known to impact diffusion of chemical species. For example, the model does not include perfusion and diffusion controlled re-oxygenation, therefore over-estimating the amount of $[O_2]$ depletion. Considering a distance of 50 μm from capillary to cell following Baish *et al.*[88], $[O_2]$ will be restored to pre-irradiation levels in ~10 s (Fig. 2 in Wilson *et al.*[89]), which could be a significant effect for lower dose rates. However, more detailed simulations taking oxygen diffusion into account show that this simplification does not have an impact on the predicted yields of $[ROO^{\cdot}]$[84].

3.4 Extension of the kinetic model to proton beams

While the vast majority of FLASH-RT studies use electron beams, recent publications have reported a FLASH effect with proton beams. Diffenderfer *et al.*[3] observed a large sparing effect against fibrogenesis of the small intestine in mice exposed to 15 to 18 Gy of 230 MeV (scattered) protons at 63-94 Gy/s. Cunningham *et al.*[90] delivered with a (scanned)

250 MeV proton beam, a uniform physical dose of 35 Gy (toxicity study) or 15 Gy (tumor control study) to the right hind leg of mice at 57 and 115Gy/s and observed that skin toxicity and leg contracture were all significantly decreased in FLASH-RT compared to CONV while both dose rates showed similar efficacy with regards to tumor growth control. This raises interesting questions of how to account in radiochemical models the different beam properties of electrons and protons (Figure 3). More specifically: *(i)* the influence of the linear energy transfer (LET) on the FLASH-RT mechanism, *(ii)* the influence of the use of a *continuous* proton beam (instead of a *pulsed* electron beam) in the case of scattered proton beam or, alternatively, the influence of the spot delivery timing in the case of pencil beam scanning and (iii) the rapid decrease of the particle fluence in the depth of the tissue, in the region of the Bragg peak. These questions are far from being settled and only some hints on way to modify the models can be suggested here.

Regarding the first question, the LET depends on the velocity of the proton and increases with penetration depth[91]: for a spread-out Bragg peak (SOBP) with 12 cm proton range and a 7 cm modulation, the LET starts from around 1 keV/μm at the entrance point in the tissues, increases slowly from 2 to 4 keV/μm in the plateau of the SOBP and then, toward the end of the proton track, increases rapidly to 14 keV/μm (see Fig. 1 in Lühr *et al.*[91]). The relative biological efficiency (RBE) is known to increase with the LET in the depth of the tissue at CONV dose rate[92]. Whether this increase is sufficient to influence the mechanism of the FLASH effect remains uncertain. While current technologies have not been developed to the extent to adequately discriminate how the FLASH effect depends on LET, such data seems likely in the near future. In this light, and given the relative inverse relationship between OER and LET, demonstration of the FLASH effect at higher LET values ($\sim \geq$ 40 keV/μm) might well provide evidence that the FLASH effect is not reliant on oxygen tension. Furthermore, obtaining the FLASH effect in the Bragg peak may in fact be entirely unnecessary, as long as the dose rate in the plateau region traversing the normal tissue is sufficiently high to elicit sparing, dose rate within the tumor becomes less concerning, as long as critical structures potentially exposed at the distal edge are below dose limiting toxicities.

To expand on the foregoing, it's important to note that the spatial LET distribution will depend on the specifics of beam delivery. The current proton FLASH-RT experiments[3] and the simulations of FLASH-RT treatment plans[93] use transmission beams, i.e. the Bragg peak is located beyond the patient (Figure 3A). In this configuration, the LET can be considered relatively constant over the irradiated volume and one could rule out the question of considering the effect of the LET in the radiochemical models. However, the transmission geometry is clearly sub-optimal as it does not use the conformality potential of the SOBP and requires instead multi-beam "arc" treatment plans to achieve conformality. Instead, one can consider that, in order to use the full potential of proton therapy, proton FLASH-RTwill be achieved in clinics with a SOBP constructed, for example, by using a conformal energy filter (CEF, also called "ridge filter")[94]: one single energy layer is delivered in pencil beam scanning (PBS) and the SOBP depth modulation is achieved by the spikes of the CEF (Figure 3B), therefore avoiding the energy layer switching time problem mentioned by Zou *et al.*[95]. In this configuration, it is worthwhile to consider the effect of the spatial variation of the LET on the predictions of the radiochemical models. The dose in the distal part of

the SOBP is deposited by a relatively larger portion of higher LET protons (see Fig. 1 in Lühr *et al.*[91]). Even at CONV dose rate, reliable biological models to relate the LET to the relative biological effectiveness (RBE) are still wanted[91], leading proton therapy treatment centers to assume a constant RBE = 1.1 throughout the irradiated volume[96]. It can therefore be a bit daring to try and model the dose-rate dependence of the biological effect of LET with the currently available data. Studies of the effect of high dose rate proton irradiation on cells located in the distal part of the Bragg peaks (where the LET increases) are therefore crucial[97]. Indeed, the outcome of these studies would determine whether one could use the FLASH effect to protect a critical structure in the distal part of the SOBP. Further elucidation of the LET versus SOBP influence of proton FLASH awaits both technological developments and biological validation of any potential changes in the *in vivo* FLASH effect.

The second question is the influence on the radiochemical models of the timing difference between electron beam and proton beams. Indeed, contrarily to electron beams which are pulsed with high instantaneous dose rate (10^6-10^7 Gy/s), proton beams deliver the dose in a single (long) “pulse” with low instantaneous dose rate (~10^2 Gy/s, see subgraph in Figure 3A). Despite the lower dose rate, the FLASH effect is still observed experimentally[3]. The radiochemical models must therefore be able to predict the existence of a FLASH effect both in the case of pulsed and continuous beams.

Additionally, to date, FLASH-RT experiments with electrons and protons involve passive scattering of the beam to irradiate the entire target volume. On the contrary, in PBS, overlapping pencil beam are sequentially shot to cover the whole field which lead to low frequency pulsed dose delivery at each voxel (subgraph in Figure 3B).

Another unknown relates to whether the FLASH effect is local, in which case the PBS approach is possible, or is it necessary to irradiate the entire tumor bed in less than 100 ms. Systematic experiments are still required to determine whether the FLASH effect occurs with spot scanning. However, there are already two promising initial reports. With X-rays, Montay-Gruel *et al.*[6] scanned a mouse at speeds around 62 mm/s through a 50 μm slit shaped synchrotron generated X-ray beam to cover a 17 mm field and achieve 10 Gy whole brain irradiation. The dose rate in each 50 μm slice was 12 kGy/s. Despite the scanning nature of the experiment, no memory loss was observed in the mice. Furthermore, Girdhani *et al.*[4] used proton PBS to deliver 15, 17.5 and 20 Gy at 1 Gy/s and 40 Gy/s for whole thorax irradiation of C57BL/6 mice. They observed a reduction in lung fibrosis at a 36 week endpoint, as well as reduced incidence of skin dermatitis and improved survival for high dose rate at 17.5 Gy but no difference between the two dose rates at 15 Gy nor 20 Gy which is confounding. While these reports suggest that FLASH effect is possible with PBS irradiation, further experimentation is clearly required to definitively establish whether the *in vivo* FLASH effect can be rigorously validated using PBS and CEF approaches.

4 DISCUSSION

The previous sections describe some of the experimental evidence in favor of and against the TOD hypothesis, that normal tissue sparing at ultrahigh dose rates is a consequence

of oxygen depletion resulting in a transient hypoxic radioprotection. While data derived *in vivo* with mice (carbogen breathing) and Zebra fish (radical scavengers)[6] suggest that local oxygen tension has a strong influence over eventual outcomes, the isoefficiency of tumor cell kill under normoxic and hypoxic conditions is less supportive. Moreover, neither direct measurements of the amount of oxygen consumption during FLASH irradiation *in vitro* and *in vivo* by optical methods[80,81] nor the observation of a FLASH effect in cells in aerated culture with DNA damage and survival as endpoints[76], lend support to the TOD hypothesis in such a way that radical self-annihilation[84] appears to be a more plausible explanation.

Literature also points to conflicting rationale based on quantitative comparison of G-values, where without chain propagating lipid reactions and/or redox chemistry facilitated by labile metals, radiolytic consumption of oxygen is insufficient to fully explain *in vivo* normal tissue protection. The field of FLASH-RT is clearly at a crossroads, as physicists, chemists and biologists seek to elucidate the mechanistic basis of the FLASH effect.

As detailed in a recent perspective[10] such factors as the intra-pulse dose rate, pulse number, pulse repetition frequency, duration of exposure and volume effects require further scrutiny for optimization of FLASH-RT parameters. Important here is the realization that despite any and all beam modifications that are currently under investigation using electrons (VHEE included), X-rays and protons, ultimate validation of beam delivery modalities will ultimately rely on *in vivo* biological validation. Thus, moving forward, publications that omit critical beam parameters do not serve the field well, as potential negative effects must be carefully scrutinized to properly place a set of given experimental conditions within the context of published literature. As detailed in the present review, a wealth of additional radiochemical investigation must be undertaken from cell-free to more complex biological system to quantify and contrast the types, yields and half-lives of the free radical species generated. As traditional radiobiology has taught us that the radiation chemistry is linear with dose, this is not likely going to be any different under FLASH-RT dose rates. However, this does not suggest that the subsequent course of downstream free radical reactions will follow similar reaction kinetics, as the yields of specific free radical species and their reaction products may follow very different paths. In particular, the balance between the direct and indirect effects in the context of the FLASH-RT is an important issue, but convincing evidence is lacking, so further investigations regarding how the OER responds to FLASH-RT are warranted. Challenges here remain, as defining these reaction pathways from cell free, to cellular to more complex biological models is not a trivial undertaking, as we have known for decades that the biological response to radiolytic damage involves many non-linear processes that are difficult to extrapolate. In the end, work derived from biological models and radiochemical investigations must put forth a series of testable hypotheses able to be conducted through careful biological experimentation. Theory is great, but the most useful models much provide parametric variables that can be manipulated to critically test validity.

The underlying mechanistic basis of FLASH-RT has yet to be elucidated, but this is also the case for the mechanistic basis underlying many of the factors confounding current clinical practice in radiation oncology. For example, radioresistant tumors, inter-individual differences and tumor recurrence remain problematic, yet radiotherapy is still used to

treat roughly 50% of all cancer cases, standing as a frontline treatment in the battle against cancer. It is for these cases that lies the promise of FLASH-RT: the capability of implementing dose rate as an adjustable parameter for therapeutic gain. It has caught the field of radiation oncology by surprise and has stimulated much excitement regarding its potential translation promise. FLASH-RT may alter the course of current standard of care more than any other technology in decades, and has changed the way many in our field have chosen to redirect and conduct their current research programs. This portends change, and whether FLASH-RT ultimately delivers on its lofty expectations remains to be seen, it has captured our imagination, stimulated new ideas and thus, remains an area worthy of further investigation.

ACKNOWLEDGMENTS

This work was supported by a grant from the NIH P01CA244091 to CLL; Walloon Region, grant No.8341 to RL; the Institut Curie, Inserm (ITMO 19 CP1223-00) and the Nanotherad IDEX (Paris-Saclay University) to VF.

DATA AVAILABILITY STATEMENT

Data sharing is not applicable to this article as no new data were created or analyzed in this study.

REFERENCES

1. Favaudon V, Caplier L, Monceau V, et al. Ultrahigh dose-rate FLASH irradiation increases the differential response between normal and tumor tissue in mice. Sci Transl Med. 2014;6:245ra293.
2. Patriarca A, Fouillade C, Auger M, et al. Experimental set-up for FLASH proton irradiation of small animals using a clinical system. Int J Radiat Oncol Biol Phys. 2018;102:619–626. [PubMed: 30017793]
3. Diffenderfer ES, Verginadis II, Kim MM, et al. Design, implementation, and in vivo validation of a novel proton FLASH radiation therapy system. Int J Radiat Oncol Biol Phys. 2020;106:440–448. [PubMed: 31928642]
4. Girdhani S, Abel E, Katsis A, et al. FLASH: A novel paradigm changing tumor irradiation platform that enhances therapeutic ratio by reducing normal tissue toxicity and activating immune pathways. Cancer Res. 2019;79 Abstract No. LB-280.
5. Hendry JH, Moore JV, Hodgson BW, Keene JP. The constant low oxygen concentration in all the target cells for mouse tail radionecrosis. Radiat Res. 1982;92:172–181. [PubMed: 7134382]
6. Montay-Gruel P, Acharya MM, Petersson K, et al. Long-term neurocognitive benefits of FLASH radiotherapy driven by reduced reactive oxygen species. Proc Natl Acad Sci USA. 2019;116:10943–10951. [PubMed: 31097580]
7. Alaghband Y, Cheeks SN, Allen BD, et al. Neuroprotection of radiosensitive juvenile mice by ultra-high dose rate FLASH irradiation. Cancers (Basel). 2020;12:1671.
8. Montay-Gruel P, Petersson K, Jaccard M, et al. Irradiation in a flash: Unique sparing of memory in mice after whole brain irradiation with dose rates above 100Gy/s. Radiother Oncol. 2017;124:365–369. [PubMed: 28545957]
9. Acharya S, Bhat N, Joseph P, Sanjeev G, Sreedevi B, Narayana Y. Dose rate effect on micronuclei induction in human blood lymphocytes exposed to single pulse and multiple pulses of electrons. Radiat Environ Biophys. 2011;50:253–263. [PubMed: 21259020]
10. Vozenin MC, Montay-Gruel P, Limoli C, Germond JF. All irradiations that are ultra-high dose rate may not be FLASH: the critical importance of beam parameter characterization and in vivo validation of the FLASH effect. Radiat Res. 2020;194:571–572. [PubMed: 32853355]

11. Montay-Gruel P, Acharya MM, Gonçalves Jorge P, et al. Hypo-fractionated FLASH-RT as an effective treatment against glioblastoma that reduces neurocognitive side effects in mice. Clin Cancer Res. 2020;27:775–784. [PubMed: 33060122]
12. Friedl AA, Prise KM, Butterworth K, Montay-Gruel P, Favaudon V. Radiobiology of the FLASH effect. Med Phys. 2021;This issue of the journal.
13. Schwarz G Über Desensibilisierung gegen Röntgen- und Radium-strahlen. Münchner Medizinische Wochenschrift. 1909;56:1217–1218.
14. Petry E Zur Kenntnis derr Bedingungen derr biologischen Wirkung der Röntgenstrahlen. Biochem Zeitschr 1923;135:353.
15. Crabtree HG, Cramer W. Action of radium on cancer cells: some factors affecting susceptibility of cancer cells to radium. Proc R Soc Lond B Biol Sci. 1933;113:238.
16. Read J Mode of action of X-ray doses given with different oxygen concentrations. Br J Radiol. 1952;25:336–338. [PubMed: 14925316]
17. Gray LH, Conger AD, Ebert M, Hornsey S, Scott OC. The concentration of oxygen dissolved in tissues at the time of irradiation as a factor in radiotherapy. Br J Radiol. 1953;26:628–648. [PubMed: 13106295]
18. Hall EJ, Amato JG. Oxygen effect and reoxygenation. In: John JR, Sutton P, Marino D, eds. Radiobiology for the radiologist. 6th edition ed. Philadelphia: Lippincott Williams & Wilkins.; 2006:85–105.
19. McKeown SR. Defining normoxia, physoxia and hypoxia in tumours. Implications for treatment response. Br J Radiol. 2014;87:20130676. [PubMed: 24588669]
20. Tallentire A, Jones AB, Jacobs GP. The radiosensitizing actions of ketonic agents and oxygen in bacterial spores suspended in aqueous and non-aqueous mlilieux. Isr J Chem. 1972;10:1185–1197.
21. Millar BC, Fielden EM, Steele JJ. A biphasic radiation survival response of mammalian cells to molecular oxygen. Int J Radiat Biol. 1979;36:177–180.
22. Ewing D, Powers EL. Irradiation of bacterial spores in water: three classes of oxygen-dependent damage. Science. 1976;194:1049–1051. [PubMed: 824733]
23. Kiefer J, Schopfer F, Luggen-Holscher J. The kinetics of the oxygen effect in yeast irradiated in dry and wet conditions. In: Rogers MAJ, Powers EL, eds. Oxygen and oxy-radicals in chemistry and biology. New York: Academic Press; 1980:293–299.
24. Adams GE, Jameson DG. Time effects in molecular radiation biology. Radiat Environ Biophys. 1980;17:95–113. [PubMed: 6768098]
25. Grimes DR, Partridge M. A mechanistic investigation of the oxygen fixation hypothesis and oxygen enhancement ratio. Biomed Phys Eng Express. 2015;1:045209. [PubMed: 26925254]
26. von Sonntag C Protection, sensitization and the oxygen effect. In: The chemical basis of radiation biology. London, Philadelphia: Taylor and Francis; 1987:pp. 295–352.
27. Howard-Flanders P, Moore D. The time interval after pulsed irradiation within which injury to bacteria can be modified by dissolved oxygen. I. A search for an effect of oxygen 0.02 second after pulsed irradiation. Radiat Res. 1958;9:422–437. [PubMed: 13591515]
28. Michael BD, Adams GE, Hewitt HB, Jones WB, Watts ME. A posteffect of oxygen in irradiated bacteria: a submillisecond fast mixing study. Radiat Res. 1973;54:239–251. [PubMed: 4574206]
29. Michael BD, Davies S, Held KD. Ultrafast chemical repair of DNA single and double strand break precursors in irradiated V79 cells. Basic Life Sci. 1986;38:89–100. [PubMed: 3741350]
30. Michael BD, Harrop HA, Maughan RL. Fast response methods in the radiation chemistry of lethal damage in intact cells. Paper presented at: Radiation Research. Proceedings of the 6th international congress on radiation research.1979; Tokyo.
31. Watts ME, Maughan RL, Michael BD. Fast kinetics of the oxygen effect in irradiated mammalian cells. Int J Radiat Biol. 1978;33:195–199.
32. Willson R The reaction of oxygen with radiation-induced free radicals in DNA and related compounds. Int J Radiat Biol. 1970;17:349–358.
33. Isildar M, Schuchmann M, Schulte-Frohlinde D, von Sonntag C. Oxygen uptake in the radiolysis of aqueous solutions of nucleic acids and their constituents. Int J Radiat Biol. 1982;41:525–533.

34. Epp ER, Weiss H, Ling CC. Irradiation of cells by single and double pulses of high intensity irradiation: oxygen sensitization and diffusion kinetics. Curr Top Radiat Res. 1976;11:201–230.
35. Michael BD, Harrop HA, Held KD. Timescale and mechanisms of the oxygen effect in irradiated bacteria. In: Rodger MAJ, Powers EL, eds. Oxygen and oxy-radicals in chemistry and biology. New York: Academic Press; 1981:285–292.
36. Slagle IR, Ratajczak E, Heaven MC, Gutman D, Wagner AF. Kinetics of polyatomic free radicals produced by laser photolysis. 4. Study of the equilibrium i-C3H7 + O2 / i-C3H7O2 between 592 and 692 K. J Am Chem Soc. 1985;107:1834–1845.
37. Slagle IR, Ratajczak E, Gutman D. Study of the thermochemistry of the C2H5 + O2 / C2H5O2 and t-C4Hg + O2 / t-C4H2O2 reactions and of the trend of alkylperoxy bond strengths. J Phys Chem Ref Data. 1986;90:402–407.
38. von Sonntag C Peroxyl radicals. In: The chemical basis of radiation biology. London, Philadelphia: Taylor and Francis; 1987:pp. 57–93.
39. von Sonntag C DNA model systems: the base moiety. In: The chemical basis of radiation biology. London, Philadelphia: Taylor and Francis; 1987:pp. 116–166.
40. Hong ISH, Carter KN, Sato K, Greenberg MM. Characterization and mechanism of formation of tandem lesions in DNA by a nucleobase peroxyl radical. J Am Chem Soc 2007;129:4089–4098. [PubMed: 17335214]
41. Bamatraf MMM, O'Neill P, Rao BSM. Redox dependence of the rate of interaction of hydroxyl radical adducts of DNA nucleobases with oxidants: consequences for DNA strand breakage. J Am Chem Soc. 1998;120:11852–11857.
42. Douki T, Rivière J, Cadet J. DNA tandem lesions containing 8-oxo-7,8-dihydroguanine and formamido residues arise from intramolecular addition of thymine peroxyl radical to guanine. Chem Res Toxicol. 2002;15:445–454. [PubMed: 11896694]
43. Cadet J, Wagner JR. DNA base damage by reactive oxygen species, oxidizing agents, and UV radiation. Cold Spring Harb Perspect Biol. 2013;5:a012559. [PubMed: 23378590]
44. San Pedro JMN, Greenberg MM. 5,6-Dihydropyrimidine peroxyl radical reactivity in DNA. J Am Chem Soc. 2014;136:3928–3936. [PubMed: 24579910]
45. von Sonntag C DNA model systems: the sugar phosphate moiety. In: The chemical basis of radiation biology. London, Philadelphia: Taylor and Francis; 1987:pp. 167–193.
46. Wilson JD, Hammond EM, Higgins GS, Petersson K. Ultra-high dose rate (FLASH) radiotherapy: silver bullet or fool's gold? Frontiers Oncol. 2020;9:1563.
47. Riahi Y, Cohen G, Shamni O, Sasson S. Signaling and cytotoxic functions of 4-hydroxyalkenals. Am J Physiol Endocrinol Metab. 2010;299:E879–886. [PubMed: 20858748]
48. Okada S Are there other target molecules? In: Altman KI, Gerber GB, Okada S, eds. Radiation biochemistry. New York: Academic Press; 1970:Vol. 1. 148–155.
49. Wolters H, Konings AW. Radiation effects on membranes. III. The effect of X irradiation on survival of mammalian cells substituted by polyunsaturated fatty acids. Radiat Res. 1982;92:474–482. [PubMed: 7178416]
50. Santana P, Pena LA, Haimovitz-Friedman A, et al. Acid sphingomyelinase-deficient human lymphoblasts and mice are defective in radiation-induced apoptosis. Cell. 1996;86:189–199. [PubMed: 8706124]
51. Kolesnick R, Fuks Z. Radiation and ceramide-induced apoptosis. Oncogene. 2003;22:5897–5906. [PubMed: 12947396]
52. Bionda C, Hadchity E, Alphonse G, et al. Radioresistance of human carcinoma cells is correlated to a defect in raft membrane clustering. Free Radic Biol Med. 2007;43:681–694. [PubMed: 17664132]
53. Corre I, Guillonneau M, Paris F. Membrane signaling induced by high doses of ionizing radiation in the endothelial compartment. Relevance in radiation toxicity. Int J Mol Sci. 2013;14:22678–22696. [PubMed: 24252908]
54. Ayala A, Muñoz MF, Argüelles S. Lipid peroxidation: production, metabolism, and signaling mechanisms of malondialdehyde and 4-hydroxy-2-nonenal. Oxid Med Cell Longev. 2014. 360438.

55. Tudek B, Zdzalik-Bielecka D, Tudek A, Kosicki K, Fabisiewicz A, Speina E. Lipid peroxidation in face of DNA damage, DNA repair and other cellular processes. Free Radic Biol Med. 2017;107:77–89. [PubMed: 27908783]
56. Pryor WA. Oxy-radicals and related species: their formation, lifetimes, and reactions. Annu Rev Physiol. 1986;48:657–667. [PubMed: 3010829]
57. Phaniendra A, Jestadi DB, Periyasamy L. Free radicals: properties, sources, targets, and their implication in various diseases. Ind J Clin Biochem. 2015;30:11–26.
58. Hruszkewycz AM, Bergtold DS. The 9-hydroxyguanine content of isolated mitochondria increases with lipid peroxidation. Mutat Res. 1252;244:123–128.
59. Park JW, Floyd RA. Lipid peroxidation products mediate the formation of 8-hydroxydeoxyguanosine in DNA. Free Radic Biol Med. 1992;12:245–250. [PubMed: 1315708]
60. Goto M, Ueda K, Hashimoto T, et al. A formation mechanism for 8-hydroxy-2'-deoxyguanosine mediated by peroxidized 2′-deoxythymidine. Free Radic Biol Med. 2008;45:1318–1325. [PubMed: 18775490]
61. Wardman P Radiotherapy using high-intensity pulsed radiation beams (FLASH): a radiation-chemical perspective. Radiat Res. 2020;194:607–617. [PubMed: 33348369]
62. Spitz DR, Buettner GR, Petronek MS, et al. An integrated physico-chemical approach for explaining the differential impact of FLASH versus conventional dose rate irradiation on cancer and normal tissue responses. Radiother Oncol. 2019;139 23–27. [PubMed: 31010709]
63. Vozenin MC, Hendry JH, Limoli CL. Biological benefits of ultra-high dose rate FLASH radiotherapy: sleeping beauty awoken. Clin Oncol (R Coll Radiol). 2019;31:407–415. [PubMed: 31010708]
64. Koch CJ. Re: Differential impact of FLASH versus conventional dose rate irradiation: Spitz et al. Radiother Oncol. 2019;139:62–63. [PubMed: 31431380]
65. Epp ER, Weiss H, Djordjevic B, Santomasso A. The radiosensitivity of cultured mammalian cells exposed to single high intensity pulses of electrons in various concentrations of oxygen. Radiat Res. 1972;52:324–332. [PubMed: 4566064]
66. Dewey DL, Boag JW. Modification of the oxygen effect when bacteria are given large doses of radiation. Nature. 1959;183:1450–1451. [PubMed: 13657161]
67. Adrian G, Konradsson E, Lempart M, Bäck S, Ceberg C, Petersson K. The FLASH effect depends on oxygen concentration. Br J Radiol. 2019;92:20190702.
68. Kessaris ND, Weiss H, Epp ER. Diffusion of oxygen in bacterial cells after exposure to high intensity pulsed electrons: theoretical model and comparison with experiment. Radiat Res. 1973;54:181–191. [PubMed: 4703882]
69. Pratx G, Kapp DS. A computational model of radiolytic oxygen depletion during FLASH irradiation and its effect on the oxygen enhancement ratio. Phys Med Biol. 2019;64:185005. [PubMed: 31365907]
70. Petersson K, Adrian G, Butterworth K, McMahon SJ. A quantitative analysis of the role of oxygen tension in FLASH radiotherapy. Int J Radiat Oncol Biol Phys. 2020;107:539–547. [PubMed: 32145319]
71. Pratx G, Kapp DS. Ultra-high dose-rate FLASH irradiation may spare hypoxic stem cell niches in normal tissues. Int J Radiat Oncol Biol Phys. 2019;105:190–192. [PubMed: 31145965]
72. Zhou G Mechanisms underlying FLASH radiotherapy, a novel way to enlarge the differentiai responses to ionizing radiation between normal and tumor tissues. Radiat Med Protect. 2020;1:35–40.
73. Spencer JA, Ferraro F, Roussakis E, et al. Direct measurement of local oxygen concentration in the bone marrow of live animals. Nature. 2014;508:269–273. [PubMed: 24590072]
74. Tsai AG, Johnson PC, Intaglietta M. Oxygen gradients in the microcirculation. Physiol Rev. 2003;83:933–963. [PubMed: 12843412]
75. Cadet J, Davies KJA, Medeiros MHG, di Mascio P, Wagner JR. Formation and repair of oxidatively generated damage in cellular DNA. Free Radic Biol Med. 2017;107:13–34. [PubMed: 28057600]

76. Fouillade C, Curras-Alonso S, Giuranno L, et al. FLASH irradiation spares lung progenitor cells and limits the incidence of radio-induced senescence. Clin Cancer Res. 2020;26:1497–1506. [PubMed: 31796518]
77. Kirby-Smith JS, Dolphin GW. Chromosome breakage at high radiation dose-rates. Nature. 1958;182:270–271. [PubMed: 13577813]
78. Schmid TE, Dollinger G, Hable V, et al. The effectiveness of 20 MeV protons at nanosecond pulse lengths in producing chromosome aberrations in human-hamster hybrid cells. Radiat Res. 2011;175:719–727. [PubMed: 21438661]
79. Jacobs G, Samuni A, Czapski G. The contribution of endogenous and exogenous effects to radiation-induced damage in the bacterial spore. Int J Radiat Biol. 1985;47:621–627.
80. Cao X, Zhang R, Esipova TV, et al. Quantification of oxygen depletion during FLASH irradiation in vitro and in vivo. Int J Radiat Oncol Biol Phys. 2021; 10.1016/j.ijrobp.2021.1003.1056.
81. Jansen J, Knoll J, Beyreuther E, et al. Does FLASH deplete oxygen? Experimental evaluation for photons, protons and carbon ions. Med Phys. 2021; 10.1002/mp.14917.
82. Rothwell BC, Kirkby NF, Merchant MJ, et al. Determining the parameter space for effective oxygen depletion for FLASH radiation therapy. Phys Med Biol. 2021;66:055020.
83. Chabi S, Van To TH, Leavitt R, et al. Ultra-high dose rate FLASH and conventional dose rate irradiation differentially affect human acute lymphoblastic leukemia and normal hematopoiesis. Int J Radiat Oncol Biol Phys. 2020;109:819–829. [PubMed: 33075474]
84. Labarbe R, Hotoiu L, Barbier J, Favaudon V. A physicochemical model of reaction kinetics supports peroxyl radical recombination as the main determinant of the FLASH effect. Radiother Oncol. 2020;153:303–310. [PubMed: 32534957]
85. Weiss H An equation for predicting the surviving fraction of cells irradiated with single pulses delivered at ultra-high dose rates. Radiat Res. 1972;50:441–452. [PubMed: 5025236]
86. Berry RJ, Hall EJ, Forster DW, Storr TH, Goodman MJ. Survival of mammalin cells exposed to X rays at ultra-high dose-rates. Br J Radiol. 1969;42:102–107. [PubMed: 4975207]
87. Mihaljevic B, Tartaro I, Ferreri C, Chatgilialoglu C. Linoleic acid peroxidation vs. isomerization: a biomimetic model of free radical reactivity in the presence of thiols. Org Biomol Chem. 2011;9:3541–3548. [PubMed: 21442126]
88. Baish JW, Stylianopoulos T, Lanning RM, et al. Scaling rules for diffusive drug delivery in tumor and normal tissues. Proc Natl Acad Sci USA. 2011;108:1799–1803. [PubMed: 21224417]
89. Wilson P, Jones B, Yokoi T, Hill M, Vojnovic B. Revisiting the ultra-high dose rate effect: implications for charged particle radiotherapy using protons and light ions. Br J Radiol. 2012;85:E933–939. [PubMed: 22496068]
90. Cunningham S, McCauley S, Vairamani K, et al. FLASH Proton Pencil Beam Scanning irradiation minimizes radiation-induced leg contracture and skin toxicity in mice. Cancers (Basel). 2021;13: 1012. [PubMed: 33804336]
91. Lühr A, von Neubeck C, Pawelke J, et al. Radiobiology of proton therapy: results of an international expert workshop. Radiother Oncol. 2018;128:56–67. [PubMed: 29861141]
92. Calugaru V, Nauraye C, Noël G, Giocanti N, Favaudon V, Mégnin-Chanet F. Radiobiological characterization of two therapeutic proton beams with different initial energy spectra used at the Institut Curie-Proton Therapy Center in Orsay. Int J Radiat Oncol Biol Phys. 2011;81:1136–1143. [PubMed: 21075549]
93. van Marlen P, Dahele M, Folkerts M, Abel E, Slotman BJ, Verbakel WF. Bringing FLASH to the clinic: treatment planning considerations for ultrahigh dose-rate proton beams. Int J Radiat Oncol Biol Phys. 2020;106:621–629. [PubMed: 31759074]
94. Simeonov Y, Weber U, Penchev B, et al. 3D range-modulator for scanned particle therapy: development, Monte Carlo simulations and experimental evaluation. Phys Med Biol. 2017;62:7075–7096. [PubMed: 28741595]
95. Zou W, Diffenderfer ES, Cengel KA, et al. Current delivery limitations of proton PBS for FLASH. Radiother Oncol. 2021;155:212–218. [PubMed: 33186682]
96. Paganetti H. Significance and implementation of RBE variations in proton beam therapy. Technol Cancer Res Treat. 2003;2:413–426. [PubMed: 14529306]

97. Calugaru V, Nauraye C, Cordelières FP, et al. Involvement of the Artemis protein in the relative biological efficiency observed with the 76-MeV proton beam used at the Institut Curie Proton Therapy Center in Orsay. Int J Radiat Oncol Biol Phys. 2014;90:36–43. [PubMed: 25195988]

98. Michaels HB, Hunt JW. A model for radiation damage in cells by direct effect and by indirect effect: a radiation chemistry approach. Radiat Res. 1978;74:23–34. [PubMed: 674566]

99. von Sonntag C Targets in radiation biology. In: The chemical basis of radiation biology. London, Philadelphia: Taylor and Francis; 1987:pp. 94–115.

100. Cadet J, Ravanat J, TavernaPorro M, Menoni H, Angelov D. Oxidatively generated complex DNA damage: tandem and clustered lesions. Cancer Lett. 2012;327:5–15. [PubMed: 22542631]

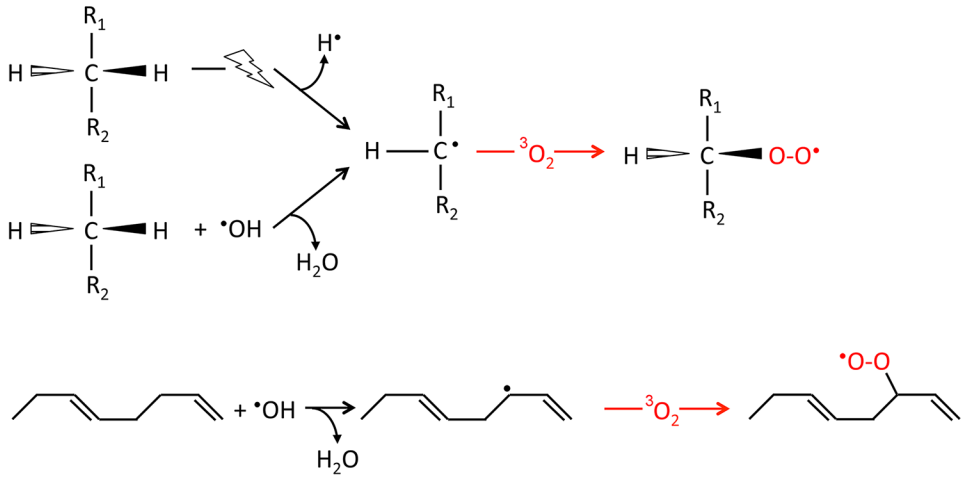

Figure 1.

Basic scheme of the direct or indirect (•OH) formation of carbon-centered radicals by hydrogen atom abstraction from an aliphatic (top) or unsaturated carbon chain (bottom) and ensuing generation of peroxyl radicals by reaction with molecular oxygen in the fundamental (triplet) state.

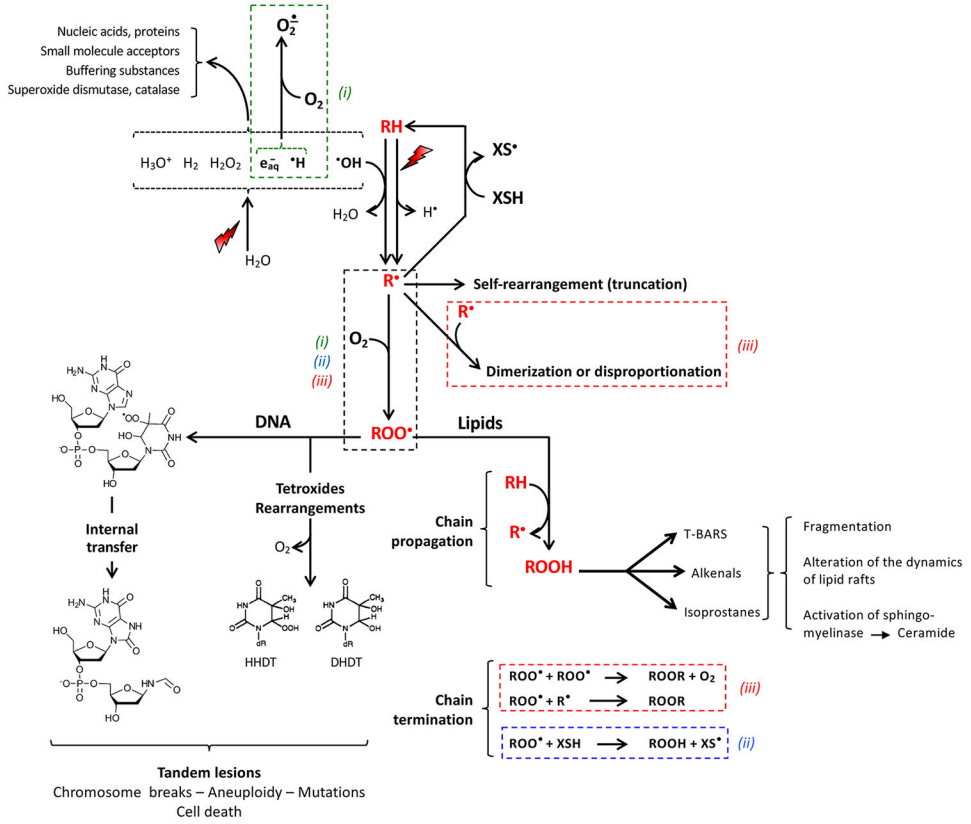

Figure 2.

General scheme summarizing the oxygen-dependent reactions leading to radiation-induced degradation of nucleic acid and lipids. The reaction starts with hydrogen atom abstraction from the carbon atom of a substrate RH either by direct energy transfer or indirectly by reaction with the •OH radical released from water radiolysis (Figure 1), approximated to ca. 30% and 70%, respectively[98,99]. Water-derived radicals are trapped by the large amount of acceptors present in cells, including oxygen generating the superoxide anion by reaction with e^-_{aq} and H• (upper left). The alkyl or allyl radical R• evolves through scavenging by hydrogen donors (XSH) including ascorbate, α-tocopherol or non-protein thiols; by internal reorganization; by bimolecular recombination; or by reaction with oxygen in the course of a diffusion-controlled reaction yielding the peroxyl radical ROO•.

In nucleic acids, peroxyl radicals may evolve following either one of two paythways. Firstly, *by s*elf-rearrangement or disproportionation via tetroxide intermediates releasing O_2 and a wealth of products. HHDT (6-hydroperoxy- 5-hydroxy-5,6-dihydrothymine) and DHDT (5,6-dihydro-5,6-dihydroxythymine) are shown as examples. Secondly, *via g*eneration of tandem lesions by reaction with vicinal nucleobases. The peroxyl radical formed at C-5 of thymidine and the end-product of its reaction with vicinal deoxyguanosine[100] is shown as an example.

In unsaturated lipids, ROO• radicals initiate a chain reaction starting with oxidation of another molecule of lipid RH with release of a new molecule of R•. Lipid peroxides decompose into by-products including alkenals, isoprostanes and thiobarbiturtic acid reactive substances (TBARS). Termination of the chain involves radical–radical annihilation,

with release of O_2 from recombination of $ROO^{\bullet}$ with itself, or reduction by thiol-like compounds.

The boxes (dotted line) underscore the main parts of the reaction network on which the hypotheses (i), (ii) and (iii) in Introduction are based. The TOD model *(i)* assumes that oxygen depletion occurs through reaction with e^{-}_{aq} and $H^{\bullet}$ and upon generation of $ROO^{\bullet}$. Model *(ii)* stems from a competition between the bimolecular recombination of $R^{\bullet}$ and the reaction $R^{\bullet} + O_2$ on the one hand, and chain termination by radical recombination involving peroxyl radicals. The cell-specific differences in the ability to detoxify from reactive oxygen species underlying hypothesis *(ii)* assumes that normal tissues are able to remove organic peroxyl radicals and peroxides more effectively than tumor tissues.

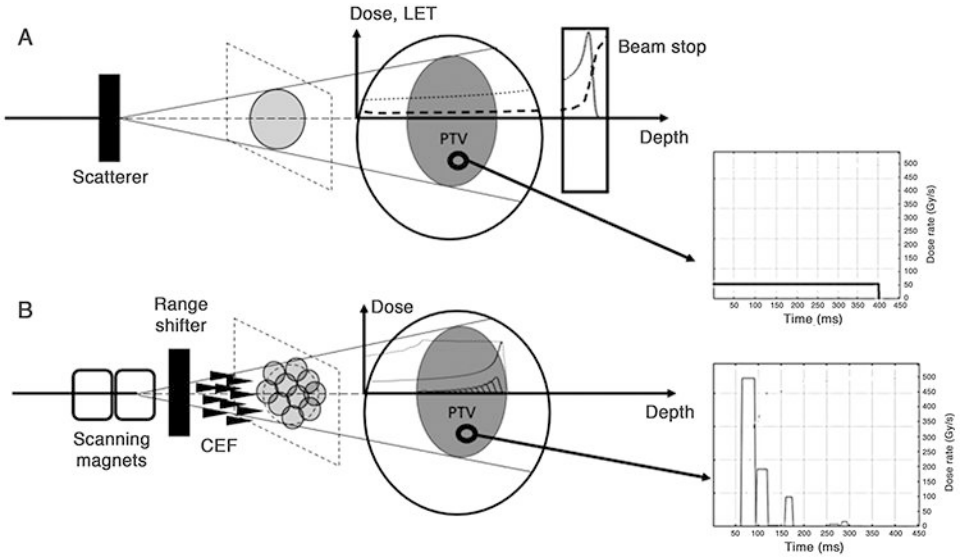

Figure 3.

A. Typical setup for a scattered proton beam in a transmission mode. The incident proton beam is scattered by the scatterer plate to cover the whole cross-section of the PTV. The depth-dose curve is represented by the dotted line. The proton energy is sufficiently high for the Bragg peak to be located outside of the patient, in a downstream beam stop. The dose deposition is relatively uniform inside the patient. The LET as a function of depth is represented by the dashed curve. The LET is constant inside the patient and significantly increases only at the Bragg peak in the beam stop. The instantaneous dose rate as a function of time at one voxel of the PTV, represented in the graph on the right, is constant.

B. Setup for pencil beam scanning (PBS) with a conformal energy filter (CEF). The incoming proton beam is scanned by two scanning magnets across the plane section of the PTV so that the full dose is deposited by sequential overlapping PBS spots. The instantaneous dose rate as a function of time at one voxel of the PTV is a sequence of dose rate “burst” corresponding to the delivery of successive PBS spots (right graph). The range shifter degrades the beam energy so that the distal fall-off of the SOBP matches the distal surface of the PTV. Each PBS spot has a circular shape and goes through one spike of the CEF which creates the SOBP (dotted curve) composed of multiple Bragg peaks (solid curves). The protons of each individual Bragg peak have a LET *vs.* depth curve similar to the one shown in Figure 3A. Inside the SOBP, the dose is deposited by protons showing a distribution of LET.

TABLE 1

Summary of the publications discussed in Section 3 that support or disprove the three hypotheses presented in the Introduction.

Hypothesis	Supporting	Not Supporting
(i) Radiation-induced transient oxygen depletion	62, 66, 67, 69, 70, 82	1, 9, 19, 73, 74, 75, 76, 77, 78, 80, 81
(ii) Cell-specific differences in the ability to detoxify	62	
(iii) Self-annihilation of radicals by recombination	9, 26, 38, 64, 84, 85, 86, 87	